ChemComm

COMMUNICATION

View Article Online
View Journal | View Issue

Cite this: *Chem. Commun.*, 2016, 52, 1174

Received 17th September 2015,
Accepted 17th November 2015

DOI: 10.1039/c5cc07813j

www.rsc.org/chemcomm

A [3Fe–3S]$^{3+}$ cluster with exclusively μ-sulfide donors†

Yousoon Lee,[a] Ie-Rang Jeon,[b] Khalil A. Abboud,[a] Ricardo García-Serres,*[c] Jason Shearer[d] and Leslie J. Murray*[a]

A [3Fe–3(μ-S)]$^{3+}$ cluster is reported in which each ferric center has a distorted trigonal pyramidal geometry, with an *S* = 1/2 ground state for the cluster and unusually anisotropic hyperfine coupling constants as determined by variable temperature magnetometry and Mössbauer spectroscopy.

Protein-bound iron–sulfur (FeS) clusters perform diverse functions in biology including electron transfer, substrate binding and activation, and analyte sensing (*e.g.*, dioxygen, nitric oxide).[1] Among FeS clusters, the iron–molybdenum cofactor (FeMoco) in nitrogenase has the unique ability to activate the triple-bond in N_2 to afford NH_3 as well as reducing a number of unsaturated substrates (*e.g.*, CO_2, C_2H_2) under ambient conditions.[2] The four iron atoms, Fe2, Fe3, Fe6, and Fe7, are linked by two μ-S^{2-} and two μ_3-S^{2-} ligands, and this face of the cluster is the proposed site for dinitrogen activation.[3] The μ-S^{2-} ligands are thought to bind protons in the reduced state.[4] To date, synthetic FeS clusters including Fe_8S_7, Fe_4NS_3, and $MoFe_3S_3$ have been reported;[5] however, μ-sulfides remain rare in synthetic iron–sulfur cluster chemistry. Relatedly, a hexagonal planar [3Fe–3S] cluster was initially proposed as the 3-Fe site of *Azotobacter vinlandii* Ferredoxin I (*Av* Fd I) based on X-ray diffraction,[6] but was later corrected to a cuboidal [3Fe–4S]$^{+}$ one.[7] Here, we report the first example of a hexagonal tri(μ-sulfido)triiron(III) cluster where all Fe and S atoms occupy the same molecular plane templated by a triethylbenzene-capped tris(β-diketiminate)cyclophane ligand.

Addition of three equivalents of $NaSCPh_3$ to Fe_3Br_3**L** (**1**)[11] resulted in the immediate formation of a dark green reaction mixture, from which crystals of Fe_3(μ-S)$_3$**L** (**2**) suitable for single crystal X-ray analysis could be obtained (82%, Scheme 1).‡ In the solid-state structure of **2** (Fig. 1), each iron center is coordinated by two diketiminate N-atoms and two μ-sulfides in a distorted trigonal pyramidal geometry (τ_4 = 0.89), reminiscent of those for the belt Fe atoms in resting-state FeMoco (τ_4 = 0.84–0.89).[8,9] This planar arrangement of the [3Fe–3S]$^{3+}$ cluster in **2** is unique in FeS chemistry; a planar Fe_3S_3 motif has only been observed for thiolate-bridged iron clusters and

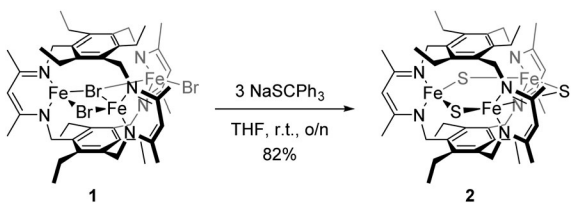

Scheme 1 Synthesis of **2**.

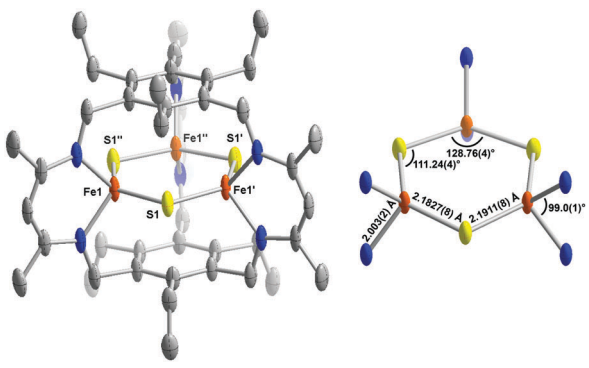

Fig. 1 Molecular structure (left) of **2** and a portion of the structure (right) depicting the bond distances and angles around the iron ions. Solvent molecules and H atoms are omitted for clarity. C, N, S and Fe atoms are depicted as gray, blue, yellow and orange ellipsoids at 55% probability.

[a] *Department of Chemistry, Center for Catalysis, University of Florida, Gainesville, FL 32611-7200, USA. E-mail: murray@chem.ufl.edu; Tel: +1 352-392-0564*
[b] *Department of Chemistry, Northwestern University, Evanston, IL 60208-3113, USA. E-mail: jeon@northwestern.edu; Tel: +1 847-491-4356*
[c] *LCBM/PMB and CEA, iRTSV/CBM/PMB and CNRS, Université Grenoble Alpes, UMR 5249, LCBM/PMB, 38000 Grenoble, France. E-mail: ricardo.garcia@cea.fr*
[d] *Department of Chemistry, University of Nevada, Reno, Reno, NV 89557, USA. E-mail: shearer@unr.edu; Tel: +1 775-784-7785*

† Electronic supplementary information (ESI) available: Full experimental procedures, spectroscopic data, cyclic and differential pulse voltammetry, and crystallographic data. CCDC 1418839. For ESI and crystallographic data in CIF or other electronic format see DOI: 10.1039/c5cc07813j

specifically the family of cyclic $Fe^{II}_3(\mu\text{-SR})_3$ compounds (R = Ph, *p*-tolyl, 2,6-$Me_2C_6H_3$).[10] The hexagonal conformation was anticipated based on the constraints imposed by the cyclophane ligand and structures of previously synthesized complexes by our group.[11,12] The iron ions in **2** are coplanar with β-diketiminate NCCCN backbone (rms deviation of fitted atoms of NCCCNFe ring = 0.01) and the benzene caps are parallel to each other with the dihedral angle of 0°, which differs from the structure of **1** in which the iron atoms are distinctly out of the NCCCN plane and there is a significant dihedral angle between the benzene caps.[11] These observations evidence a less distorted structure for **2** as compared with **1**, consistent with the smaller covalent radius of sulfide *versus* that of bromide (Fig. S1, ESI†). In comparison with $Fe^{II}_3(NH_2)_3\mathbf{L}$, which contains a similar planar Fe_3X_3 unit, the shorter Fe–N_L (N_L = N-atom on nacnac arm) bond distances (2.003(2) Å) and larger bite angle ($\angle N_L$–Fe–N_L = 99.0(1)°) in **2** than those in $Fe^{II}_3(NH_2)_3\mathbf{L}$ (2.023(2)–2.038(2) Å, 96.08(8)–96.29(8)°) agree with iron(III) centers in **2**.[12] Similarly, the Fe–S bond distances in **2** (2.1827(8)–2.1911(8) Å) are contracted relative to those in the S^{2-}-bridged bis(β-diketiminatoiron(II)) compound ($L^{Me}FeSFeL^{Me}$ where L^{Me} = [HC(C(Me)N[2,6-diisopropylphenyl])$_2$]$^-$, 2.250(2)–2.346(2) Å).[13] In comparison to the $[3Fe\text{–}4S]^+$ clusters in *Desulfovibrio gigas* ferredoxin II,[14] *Av* Fd I,[7b,15] and inactive aconitase,[16] the Fe^{III}–μS distances are slightly longer (2.21–2.33 Å) in the oxidized enzyme clusters.

The three iron atoms in **2** are ferric and high-spin as are those in cuboidal $[3Fe\text{–}4S]^+$ clusters from as-isolated aconitase, *Desulfovibrio gigas* Ferredoxin II, or pyruvate formate-lyase activating enzyme. The coupling between the three S_{Fe} = 5/2 ferric ions in the enzyme clusters is usually described with the exchange Hamiltonian: $H_{ex} = J_{12}S_1\cdot S_2 + J_{23}S_2\cdot S_3 + J_{13}S_1\cdot S_3$. The near-perfect C_3 symmetry of the [3Fe–4S] clusters implies $J_{12} \approx J_{23} \approx J_{13}$, resulting in two low-lying S_{total} = 1/2 states. The EPR spectra of the $[3Fe\text{–}4S]^+$ clusters are rhombic and centered around $g \approx 2.01$. The observed large line broadenings in these spectra are attributed to *g*-strain or to the fine structure of the Fe centers (*D*/*J*-strain).[17] The magnetic Mössbauer spectra of these clusters also display broad absorptions. These spectra can be modelled as three distinct iron sites with an S_{total} = 1/2 ground state. The broad Mössbauer absorptions were interpreted either as large anisotropies of the hyperfine coupling tensors,[18] or through the presence of *J*-strain.[19] Additionally, Münck and coworkers employed a model that invokes antisymmetric exchange to explain the broad Mössbauer spectra and the *g*-value shifts observed in the EPR spectra of some $[3Fe\text{–}4S]^+$ clusters.[20] We sought to compare the spectroscopic properties of **2** with those of the enzyme $[3Fe\text{–}4S]^+$ clusters to probe the effect, if any, of cluster geometry.

Variable temperature magnetic susceptibility data were collected on a polycrystalline sample of **2**·$2C_6H_6$ (Fig. 2). These data were not satisfactorily fit using an equilateral model (*i.e.*, $J_{12} = J_{23} = J_{13}$), and required an isosceles elongation with $J_{12} = J_{23} = 158.4\ cm^{-1}$ and $J_{13} = 187.4\ cm^{-1}$ (Fig. 2). These values are noticeably smaller than those observed between ferric sites in $[2Fe\text{–}2S]^{2+}$ clusters,[21] or in $[3Fe\text{–}4S]^+$ clusters in proteins,[22] and could arise from the longer Fe···Fe distances

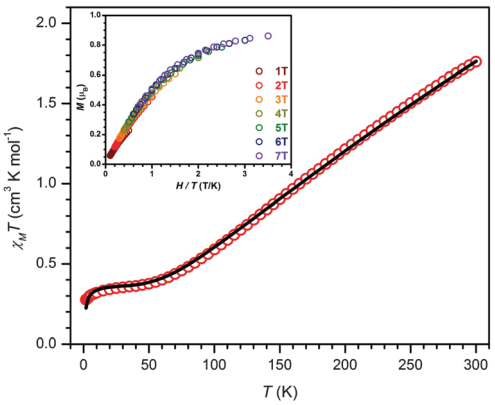

Fig. 2 Variable-temperature dc magnetic susceptibility plot for **2**·$2C_6H_6$ in a 1000 Oe applied field (red circles). A fit (black solid line) to the data yielded intramolecular magnetic exchange coupling constants $J_{12} = J_{23} = 158.4\ cm^{-1}$, and $J_{13} = 187.4\ cm^{-1}$ with fixed $g = 2$. Our simulation required inclusion of a weak intermolecular coupling term, zJ', of 3.16 cm^{-1}.[13,14] (inset) Plot of magnetization *vs.* *H*/*T* at the indicated dc fields at low temperatures. The saturating magnetization toward $M = 1\ \mu_B$ confirms the spin ground state S = 1/2 as does the molecular magnetic susceptibility of 0.38 cm^3 K mol^{-1} at 50 K (expected value of 0.375 cm^3 K mol^{-1} with $g = 2$).

(~3.6 Å in **2** *vs.* ~2.7 Å) and the more obtuse Fe–S–Fe angles than in the $[2Fe\text{–}2S]^{2+}$ and $[3Fe\text{–}4S]^+$ clusters, which should result in reduced orbital overlap. Also, the difference J_{13}–J_{12} of 29 cm^{-1} is unusually high for a ferric trimer with approximate C_3 symmetry. X-band EPR spectrum of **2** in a frozen toluene solution at 5 K showed a rhombic signal with $g \sim 2$ (Fig. S2, ESI†). We obtained a good simulation of the spectrum with an S = 1/2 spin Hamiltonian with g = 1.989, 2.006, and 2.013 and *g*-strain = 0.0291, 0.0177, 0.004. The narrow spread of *g*-values makes the spectrum very similar to "type 1" $[3Fe\text{–}4S]^+$ clusters, such as aconitase or *Av*-Fd I. For these $[3Fe\text{–}4S]^+$ clusters, the mechanism of antisymmetric exchange is not large enough to have an effect on *g*-value distribution.[20,23]

The zero-field Mössbauer spectrum of **2** at 4.2 K shows a single quadrupole doublet with δ = 0.29 mm s^{-1} and ΔE_Q = 1.34 mm s^{-1} (Fig. 3), consistent with approximately equivalent Fe(III) centers. Whereas the isomer shift is typical for ferric ions in FeS clusters,[24] the quadrupole splitting for **2** is much larger than that of iron(III) in related clusters in metalloenzymes (<1 mm s^{-1}). This difference is attributed to

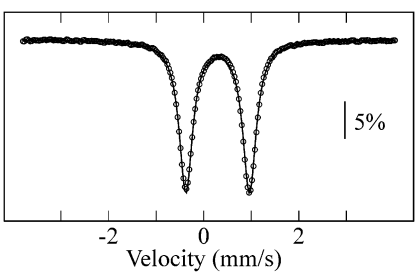

Fig. 3 Zero-field 4.2 K Mössbauer spectrum of **2**. The circles represent the experimental data points, while the solid line is a theoretical simulation with a symmetric quadrupole doublet with parameters: δ = 0.29 mm s^{-1}, ΔE_Q = 1.34 mm s^{-1}, $\Gamma_{(FWHM)}$ = 0.34 mm s^{-1}.

axial distortion at the Fe centers, induced by the mixed N_2S_2 ligand environment and the constrained and large S–Fe–S bond angles of 128.76(4)°. Spectra recorded in parallel applied magnetic fields are indicative of an S = 1/2 ground state. Contrary to the spectra of $[3Fe–4S]^+$ clusters, which display symmetric absorptions, applied field spectra of **2** are highly asymmetric. We could not reproduce the spectra of **2** with isotropic hyperfine tensors according to the spin-coupling model of Kent *et al.*,[24a] and applying a distribution of $\mathbf{A_i}$ based on *J*-strain[19] did not improve the fit. The reason for the poor simulations afforded by these models is that, although a *J* distribution reproduces the line broadening, it cannot render the observed asymmetry of the spectra. As noted by Münck and coworkers,[20] including antisymmetric exchange[25] has a similar effect to *J* distribution in broadening the spectra, but their simulations always yield symmetric spectra. We were only able to reproduce the asymmetry of our spectra by using $\mathbf{A_i}$ tensors that are extremely anisotropic (Table S1, ESI†). Although some anisotropy (∼15%) in $\mathbf{A_i}$ has been determined for some $[3Fe–4S]^+$ clusters,[26,27] high-spin ferric ions (with spherically symmetric *d*-electron distributions) are not expected to yield extremely anisotropic $\mathbf{A_i}$ tensors like those determined for **2**. Moreover, our calculated a_{test} value[28] is positive (Table S1, ESI†), which contradicts the values of ∼−20 MHz determined for all other triiron(III) clusters. To shed light on the electronic structure of **2**, we performed DFT calculations (*vide infra*), which suggested that two iron(III) centers are approximately equivalent, whereas the third is unique. We therefore simulated the Mössbauer spectra with two components with one accounting for twice the absorption of the other (Fig. S3 and Table S1, ESI†), and obtained an acceptable fit. Although we do not fully understand the reason for such anisotropic **A** tensors, the mixed N/S coordination sphere and the constrained structural metrics of **2** (*e.g.*, co-planarity of Fe and S atoms, obtuse S–Fe–S angles) likely play a crucial role.

Attempts to calculate the electronic structure of **2** using different DFT functionals (BP86, PBE0, B3LYP, mPWPW91, and B2PLYP), even when the broken symmetry approximation (BS) was employed, failed to correctly describe the nature of the iron-centers. In all cases, the electronic structure predicted one non-equivalent iron center with a localized unpaired spin, and strong antiferromagnetic coupling between the two other spins ($J > 2000$ cm^{-1}). The calculated Mössbauer parameters (δ and ΔE_Q) implied inequivalent iron-centers, not consistent with experiment. NEVPT2/CAS-SCF(5,6)/tzvp level calculations suggested the reason for these observations; the ground state wave function of **2** possesses significant multi-determinantal character. The resulting ground state wave function is described as an admixture of the LUMO (0.671) and SOMO (0.382) with the lower energy orbitals having near double occupancies (1.999 and 2.000) and the two higher energy orbitals being virtually unfilled (0.001) (Fig. 4). The resulting spin-density is evenly distributed over the three iron atoms, which correlates well with the two equivalent $\mathbf{A_{iso}}$ determined from Mössbauer (Table S1, ESI†). At this level of theory, we find an energy gap between the ground doublet and first excited doublet of 82.0 cm^{-1}. This gap is surprisingly large, considering that the two doublets are degenerate in a simple HDVV model based on an equilateral triangle geometry. However, it is consistent with our fit of the magnetic data, which implies an energy gap of $3(J_{13}–J_{12})$ = 87 cm^{-1}. The good agreement with the magnetic data is an indication that the NEVPT2 level calculation adequately describes the electronic structure of the two low-lying doublet states of the complex, despite the use of a minimal active-space. Others have used significantly larger active spaces to successfully describe the low-energy spectra of [2Fe–2S] and [4Fe–4S] clusters.[29] Our analysis is preliminary, and more detailed calculations are ongoing.

Cyclic (CV) and differential pulse (DPV) voltammograms were recorded for **2** in various solvents. In all cases, we observed a redox couple at ∼−1.55 V *vs.* Fc/Fc$^+$ in which the cathodic wave is broad relative to the anodic one (Fig. S4, S6 and S8, ESI†). In addition, the reductive wave observed by DPV is also broader than expected for a reversible one-electron process (Fig. S5, ESI†), and likely comprises two overlapping reduction events as a shoulder is clearly observed for data collected in DME or THF (Fig. S7 and S9, ESI†). This pseudo-reversible redox process is tentatively assigned as cluster-based by analogy to other synthetic and enzymatic FeS clusters.[5a,21b,30] These redox waves were absent in data collected on pristine electrolyte solutions and using electrodes that were previously used to repeatedly redox cycle a solution of **2**. Ongoing work aims to clarify the nature of these redox processes and to isolate and evaluate the reactivity of the reduced cluster(s).

In conclusion, we report the first example of a $[3Fe–3(\mu\text{-}S)]^{3+}$ cluster (**2**) for which the coordination mode of the chalcogenide

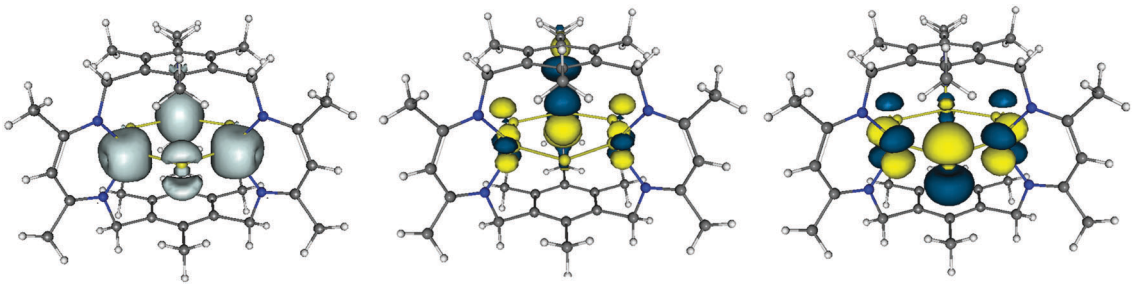

Fig. 4 Spin density plot of **2** (left) and isosurface (0.05 a.u.) plots of the partially filled MOs that comprise the leading configurations of the ground state wavefunction for **2** (SOMO middle and LUMO right).

is dictated by the cyclophane ligand. The Mössbauer spectra of **2** confirm the cluster as containing only high-spin ferric ions. Applied-field Mössbauer and X-band EPR spectra, and the temperature-dependent magnetic susceptibility support an S_{total} = 1/2 ground state for **2**. The unique planar structure of this FeS cluster confers it particular electronic properties that are reflected in the large difference between the exchange coupling constants, in its large ΔE_Q, and in its extremely anisotropic hyperfine tensor, as determined from our Mössbauer analysis. The $[3Fe–3S]^{3+}$ in **2** can be reduced electrochemically, and synthesis and characterization of chemically reduced complexes of **2** and the reactivity of the species are under active investigation.

The authors acknowledge the University of Florida (LJM, KAA), ACS Petroleum Research Fund (52704-DNI3 to LJM), National Science Foundation (CHE-1464876, CHE-0821346 (KAA), CHE-1362662 (JSS) and CHE-1048604 (LJM)), Labex ARCANE (ANR-11-LABX-0003-01 (RGS)), Northwestern University (IRJ), the International Institute for Nanotechnology (IRJ), and the Initiative for Sustainability and Energy at Northwestern (ISEN; Booster Award 10033416 (IRJ)). The authors also thank U. Twahir and Prof. A. Angerhofer for help collecting EPR data, and Prof. T. D. Harris for use of his SQUID magnetometer.

Notes and references

‡ (**2**): $C_{69}H_{87}N_6S_3Fe_3$, M_r = 1264.17, hexagonal, $P6_3/m$, a = 16.844(1) Å, b = 16.844(1) Å, c = 12.6713(8) Å, α = 90°, β = 90°, γ = 120°, V = 3113.6(4) Å^3, Z = 2, ρ_{calcd} = 1.348 mg m^{-3}, μ = 0.837 mm^{-1}, R_1 = 0.0444, wR_2 = 0.1218, GOF = 1.041.

1 (*a*) T. Rouault, *Iron–Sulfur Clusters in Chemistry and Biology*, Walter de Gruyter GmbH & Co KG, 2014; (*b*) P. Venkateswara Rao and R. H. Holm, *Chem. Rev.*, 2004, **104**, 527–560; (*c*) J. C. Crack, J. Green, A. J. Thomson and N. E. L. Brun, *Acc. Chem. Res.*, 2014, **47**, 3196–3205; (*d*) D. C. Johnson, D. R. Dean, A. D. Smith and M. K. Johnson, *Annu. Rev. Biochem.*, 2005, **74**, 247–281; (*e*) M. S. Koay, M. L. Antonkine, W. Gärtner and W. Lubitz, *Chem. Biodiversity*, 2008, **5**, 1571–1587.

2 (*a*) I. Dance, *Chem. Commun.*, 2013, **49**, 10893–10907; (*b*) M. J. Dilworth, *Biochim. Biophys. Acta, Gen. Subj.*, 1966, **127**, 285–294; (*c*) H.-I. Lee, R. Y. Igarashi, M. Laryukhin, P. E. Doan, P. C. Dos Santos, D. R. Dean, L. C. Seefeldt and B. M. Hoffman, *J. Am. Chem. Soc.*, 2004, **126**, 9563–9569; (*d*) L. C. Seefeldt, Z.-Y. Yang, S. Duval and D. R. Dean, *Biochim. Biophys. Acta, Bioenerg.*, 2013, **1827**, 1102–1111; (*e*) Z.-Y. Yang, V. R. Moure, D. R. Dean and L. C. Seefeldt, *Proc. Natl. Acad. Sci. U. S. A.*, 2012, **109**, 19644–19648; (*f*) L. C. Seefeldt, M. E. Rasche and S. A. Ensign, *Biochemistry*, 1995, **34**, 5382–5389; (*g*) S. Shaw, D. Lukoyanov, K. Danyal, D. R. Dean, B. M. Hoffman and L. C. Seefeldt, *J. Am. Chem. Soc.*, 2014, **136**, 12776–12783; (*h*) L. E. Roth and F. A. Tezcan, *J. Am. Chem. Soc.*, 2012, **134**, 8416–8419.

3 (*a*) B. M. Barney, R. Y. Igarashi, P. C. D. Santos, D. R. Dean and L. C. Seefeldt, *J. Biol. Chem.*, 2004, **279**, 53621–53624; (*b*) P. C. Dos Santos, R. Y. Igarashi, H.-I. Lee, B. M. Hoffman, L. C. Seefeldt and D. R. Dean, *Acc. Chem. Res.*, 2005, **38**, 208–214.

4 (*a*) B. M. Hoffman, D. Lukoyanov, D. R. Dean and L. C. Seefeldt, *Acc. Chem. Res.*, 2013, **46**, 587–595; (*b*) B. M. Hoffman, D. Lukoyanov, Z.-Y. Yang, D. R. Dean and L. C. Seefeldt, *Chem. Rev.*, 2014, **114**, 4041–4062.

5 (*a*) S. C. Lee, W. Lo and R. H. Holm, *Chem. Rev.*, 2014, **114**, 3579–3600; (*b*) Y. Ohki, Y. Ikagawa and K. Tatsumi, *J. Am. Chem. Soc.*, 2007, **129**, 10457–10465; (*c*) X.-D. Chen, W. Zhang, J. S. Duncan and S. C. Lee, *Inorg. Chem.*, 2012, **51**, 12891–12904; (*d*) X.-D. Chen, J. S. Duncan, A. K. Verma and S. C. Lee, *J. Am. Chem. Soc.*, 2010, **132**, 15884–15886; (*e*) S. Ohta, Y. Ohki, T. Hashimoto, R. E. Cramer and K. Tatsumi, *Inorg. Chem.*, 2012, **51**, 11217–11219; (*f*) J. Han, M. Koutmos, S. A. Ahmad and D. Coucouvanis, *Inorg. Chem.*, 2001, **40**, 5985–5999; (*g*) M. A. Tyson and D. Coucouvanis, *Inorg. Chem.*, 1997, **36**, 3808–3809; (*h*) J. Han, K. Beck, N. Ockwig and D. Coucouvanis, *J. Am. Chem. Soc.*, 1999, **121**, 10448–10449.

6 (*a*) D. Ghosh, S. O'Donnell, W. Furey Jr., A. H. Robbins and C. D. Stout, *J. Mol. Biol.*, 1982, **158**, 73–109; (*b*) D. Ghosh, W. Furey, S. O'Donnell and C. D. Stout, *J. Biol. Chem.*, 1981, **256**, 4185–4192.

7 (*a*) C. D. Stout, *J. Biol. Chem.*, 1988, **263**, 9256–9260; (*b*) C. D. Stout, *J. Mol. Biol.*, 1989, **205**, 545–555.

8 T. Spatzal, M. Aksoyoglu, L. Zhang, S. L. A. Andrade, E. Schleicher, S. Weber, D. C. Rees and O. Einsle, *Science*, 2011, **334**, 940.

9 L. Yang, D. R. Powell and R. P. Houser, *Dalton Trans.*, 2007, 955–964.

10 M. A. Whitener, J. K. Bashkin, K. S. Hagen, J. J. Girerd, E. Gamp, N. Edelstein and R. H. Holm, *J. Am. Chem. Soc.*, 1986, **108**, 5607–5620.

11 G. L. Guillet, F. T. Sloane, D. M. Ermert, M. W. Calkins, M. K. Peprah, E. S. Knowles, E. Čižmár, K. A. Abboud, M. W. Meisel and L. J. Murray, *Chem. Commun.*, 2013, **49**, 6635–6637.

12 Y. Lee, F. T. Sloane, G. Blondin, K. A. Abboud, R. García-Serres and L. J. Murray, *Angew. Chem., Int. Ed.*, 2015, **54**, 1499–1503.

13 J. Vela, S. Stoian, C. J. Flaschenriem, E. Münck and P. L. Holland, *J. Am. Chem. Soc.*, 2004, **126**, 4522–4523.

14 C. R. Kissinger, L. C. Sieker, E. T. Adman and L. H. Jensen, *J. Mol. Biol.*, 1991, **219**, 693–715.

15 C. D. Stout, *J. Biol. Chem.*, 1993, **268**, 25920–25927.

16 A. H. Robbins and C. D. Stout, *Proteins: Struct., Funct., Bioinf.*, 1989, **5**, 289–312.

17 (*a*) B. Guigliarelli, C. More, P. Bertrand and J. P. Gayda, *J. Chem. Phys.*, 1986, **85**, 2774–2778; (*b*) B. Guigliarelli, P. Bertrand, C. More, R. Haser and J. P. Gayda, *J. Mol. Biol.*, 1990, **216**, 161–166.

18 (*a*) M. H. Emptage, T. A. Kent, B. H. Huynh, J. Rawlings, W. H. Orme-Johnson and E. Münck, *J. Biol. Chem.*, 1980, **255**, 1793–1796; (*b*) B. H. Huynh, J. J. Moura, I. Moura, T. A. Kent, J. LeGall, A. V. Xavier and E. Münck, *J. Biol. Chem.*, 1980, **255**, 3242–3244.

19 C. Krebs, T. F. Henshaw, J. Cheek, B. H. Huynh and J. B. Broderick, *J. Am. Chem. Soc.*, 2000, **122**, 12497–12506.

20 Y. Sanakis, A. L. Macedo, I. Moura, J. J. G. Moura, V. Papaefthymiou and E. Münck, *J. Am. Chem. Soc.*, 2000, **122**, 11855–11863.

21 (*a*) W. Lovenberg, *Molecular Properties*, Elsevier, 2012; (*b*) J. Ballmann, X. Sun, S. Dechert, E. Bill and F. Meyer, *J. Inorg. Biochem.*, 2007, **101**, 305–312.

22 A. L. Macedo, I. Moura, J. J. G. Moura, J. Le Gall and H. B. Hanh, *Inorg. Chem.*, 1993, **32**, 1101–1105.

23 Y. V. Rakitin, Y. V. Yablokov and V. V. Zelentsov, *J. Magn. Reson.*, 1981, **43**, 288–301, DOI: 10.1016/0022-2364(81)90039-1.

24 (*a*) T. A. Kent, B. H. Huynh and E. Münck, *Proc. Natl. Acad. Sci. U. S. A.*, 1980, **77**, 6574–6576; (*b*) H. Beinert, R. H. Holm and E. Münck, *Science*, 1997, **277**, 653–659; (*c*) A. Albers, S. Demeshko, S. Dechert, C. T. Saouma, J. M. Mayer and F. Meyer, *J. Am. Chem. Soc.*, 2014, **136**, 3946–3954; (*d*) E. Bill, in *ICAME 2011*, ed. Y. Yoshida, Springer Netherlands, 2013, pp. 287–295.

25 V. E. Fainzil'berg, M. I. Belinskii and B. S. Tsukerblat, *Mol. Phys.*, 1981, **44**, 1195–1213.

26 A. L. Macedo, I. Moura, K. K. Surerus, V. Papaefthymiou, M. Y. Liu, J. LeGall, E. Münck and J. J. Moura, *J. Biol. Chem.*, 1994, **269**, 8052–8058.

27 P. E. Doan, C. Fan and B. M. Hoffman, *J. Am. Chem. Soc.*, 1994, **116**, 1033–1041.

28 J.-M. Mouesca, L. Noodleman, D. A. Case and B. Lamotte, *Inorg. Chem.*, 1995, **34**, 4347–4359.

29 S. Sharma, K. Sivalingam, F. Neese and G. K.-L. Chan, *Nat. Chem.*, 2014, **6**, 927–933.

30 (*a*) H. Ogino, S. Inomata and H. Tobita, *Chem. Rev.*, 1998, **98**, 2093–2122; (*b*) B. V. DePamphilis, B. A. Averill, T. Herskovitz, L. Que and R. H. Holm, *J. Am. Chem. Soc.*, 1974, **96**, 4159–4167; (*c*) A. Albers, T. Bayer, S. Demeshko, S. Dechert and F. Meyer, *Chem. – Eur. J.*, 2013, **19**, 10101–10106.